Proper E-cadherin membrane location in colon requires Dab2 and it modifies by inflammation and cancer

María D. Vazquez-Carretero[1]*, Pablo García-Miranda[1]*, María S. Balda[2], Karl Matter[2], Anunciación A. Ilundáin[1], María J. Peral[1]

[1] Departamento de Fisiología, Facultad de Farmacia, Universidad de Sevilla, Spain
[2] Department of Cell Biology, Institute of Ophthalmology, University College London, United Kingdom

*Corresponding authors: Pablo García Miranda and María D. Vazquez-Carretero
Departamento de Fisiología, Facultad de Farmacia, Universidad de Sevilla, Spain
C/ Profesor García González, nº 2
41012 Sevilla, Spain.
Telephone: 34 954556777
Email address: pgarcia2@us.es; mvazquez1@us.es

Acknowledgements

The work was supported by a Grant from the Junta de Andalucía (CTS 5884) and by a fellowship from The European Molecular Biology Organization (EMBO; ASTF45-2012) to M.D. Vazquez-Carretero. Immunofluorescence images were obtained in the "Centro de Investigación Tecnología e Innovación de la Universidad de Sevilla" (CITIUS), Universidad de Sevilla. We also thank "Biobanco Hospital Virgen del Rocío-IBIS (Biobanco SSPA y Red de Biobanco-ISCCII-PT13/0010/0056)" for providing us the human samples.

ABSTRACT

We reported Disabled 2 (Dab2) involvement in milk macromolecules endocytosis in suckling rat intestine. Here, we discovered that Dab2 is mainly at the villi apical cell membrane in the suckling and at both, apical and lateral membrane, along the crypt-villus axis in adult mouse small intestine. In the colon of suckling and adult mouse, and of adult human, Dab2 localized only at the lateral crypt cell membranes, where it colocalized with E-cadherin. In Caco-2 cells, depletion of Dab2, by RNA interference, led to E-cadherin internalization indicating that E-cadherin location at the membrane requires of Dab2. Then, we assessed Dab2/E-cadherin colocalization in mice colon under dextran sulfate sodium (DSS)-induced inflammation. Dab2/E-cadherin colocalization increased by day 3 of DSS-treatment, decreasing thereafter as colitis progressed from 3 to 6 and 9 days. In agreement, in human colon, increased Dab2/E-cadherin colocalization was found in mild and severe ulcerative colitis and in polyps, but reduced and even absent epithelial Dab2 expression was observed in adenocarcinoma. The latter is accompanied by E-cadherin delocalization. The decrease in epithelial Dab2 expression preceded that of E-cadherin. The data suggest that Dab2, by inhibiting E-cadherin internalization, could stabilize AJs and its absence from the epithelial cells may contribute to development of colon inflammation and cancer.

Keywords: Dab2, E-cadherin, junctions, colon, inflammation, cancer

Introduction

The intestinal epithelium acts as selectively permeable barrier allowing the absorption of nutrients and simultaneously preventing the entry of luminal pathogens into the organism. The apical junction complex (AJC), composed of tight (TJ) and adherens (AJ) junctions, connect adjacent cells (see [1] for a review). AJ consist of the transmembrane proteins E-cadherin and nectins and of cytosolic proteins, such as p-120, β-catenin and α-catenin, which mediate E-cadherin anchorage to the actomyosin cytoskeleton. The TJ transmembrane proteins include claudins, occludin, JAM and marvelD3 and among the cytosolic proteins is zonula occludens-1 (ZO-1) that interacts with transmembrane proteins and with the actin cytoskeleton, giving stability to the junction. The formation of TJ is preceded by and depends on AJ formation (see [2] for a review). The AJC are dynamic structures where new proteins are supplied to and recycled from the junctions and its maintenance is crucial for both, keeping the epithelium polarity and the intestinal barrier integrity. The alteration of the intestinal barrier integrity leads to the development of intestinal and extraintestinal diseases (see [3, 4] for review).

Disabled 2 (Dab2) is a cytoplasmic adaptor protein [5], that by interacting simultaneously with cytosolic and membrane proteins, plays multiple physiological roles through endocytosis, such as polarized cellular trafficking of membrane receptors, adhesion molecules as E-cadherin, signalling molecules, the cystic fibrosis transmembrane conductance regulator in intestine, among others (see [6] for a review); it participates in Gap junctions endocytosis [7] and in immune responses modulation (see [6] for a review), and it is required for epithelial cells surface positioning in the endoderm [8] and for endosome recycling [9]. Dab2 has also been considered a tumour suppressor because its expression is reduced or lost in several human cancer types (see [6] for a review), including colon cancer [10]. This reduction appears to contribute to epithelial-mesenchymal transition (EMT) in breast, cervical and ovarian cancer cells [11–13]. The evidence regarding the role of Dab2 in inflammation is contradictory and focused on immune cells (see [6] for a review).

We reported that the Dab2 located at the apical membrane of the suckling rat small intestine epithelium might mediate intestinal endocytosis of milk macromolecules [14]. In the current study, we discovered that Dab2 is involved in E-cadherin localization at cell-cell junctions in Caco-2 cells and that Dab2 and E-cadherin colocalization is disrupted in colon inflammation and adenocarcinoma in mouse and human *ex vivo*.

Materials and methods

Materials

The antibodies and their dilutions used are given in supplementary Materials.

Cell culture

Stable human epithelial colorectal adenocarcinoma cells (Caco-2) were grown in DMEM (Dulbecco´s Modified Eagle Medium) supplemented with 20% of fetal calf serum and in the presence of 100 U/ml penicillin and 100 µg/ml streptomycin at 37°C and in a 5% CO_2 atmosphere. Cells were cultured and plated for experiments as previously described [15].

Depletion of Dab2 in Caco-2 cells

RNA-mediated interference (RNAi) experiments were used. Caco-2 cells were cultured to 80% confluence and transfected with either a pool of siRNAs specific for Dab2 (siDab2) or a non-targeting control siRNAs. In both cases, the total final siRNA concentration was 0.2 µM. For the transfection, Interferin transfection reagent (Polyplus Transfection) was used according to the manufacturer's instructions. The siRNAs were purchased by Sigma-Aldrich. The sequences of the specific siRNAs for Dab2 were (5´…3´): CAAUCGACACCUUCUUCGU and ACGAAGAAGGUGUCGAUUG; CAUGAUGACUUUGAUGCUA and UAGCAUCAAAGUCAUCAUG. 3 days after transfection, samples were collected and processed either for immunofluorescence, western blot or paracellular gate permeability.

Analysis of the paracellular gate

Ion permeability was determined by measuring transepithelial electrical resistance (TER). A silver/silver-chloride electrode was used to determine the voltage deflection induced by an alternating current square wave current (±20 µA at 12.5 Hz) using an epithelial voltohmmeter (EVOM; World Precision Instruments) as previously described [16]. Briefly, either control or siDab2 Caco-2 cells were plated on transwell filters and allowed to form confluent monolayer in normal medium. TER was measured after 24, 30, 48 and 60 h of culture and results are expressed in ohm x cm^2. Paracellular permeability of hydrophilic tracers was monitored by measuring the transmonolayer flux of either 4 kDa FITC- or 70 kDa Rhodamine B-conjugated dextran over 2, 4, 6 and 8 h. Fluorescence was then determined with a FLUOstar OPTIMA microplate reader (BMGLabTech, Offenburg, Germany).

Animals and experimental colitis

C57BL/6 mice of 8 day (suckling) and 3 month-old (adult) were housed in a 12:12 light/dark cycle and fed *ad libitum* with normal rodent diet (Harlan Ibérica S.L.) and free access to tap water. They were humanely handled and sacrificed by cervical dislocation according with the guidelines of the European Union Council (Directive 2010/63/UE).

Colitis was induced in 3 month-old mice by drinking water containing 3% (wt/vol) dextran sulphate sodium (DSS, MW 40 kDa; TdB Consultancy) during 3, 6 or 9 days. Tap water was administered to DSS-untreated animals. Following sacrifice, the colon was removed, washed with ice-cold saline solution and fixed by overnight incubation with phosphate buffer saline (PBS) (in mM, 137 NaCl, 2.7 KCl, 10 Na_2HPO_4 and 1.8 KH_2PO_4 pH 7.4) containing 4% para-formaldehyde for histological analysis. The progression of the colon inflammation was assessed by determining disease activity index (DAI), histological score and by the mRNA levels of the pro-inflammatory cytokines IL-1β and TNFα, as described [17]. For DAI evaluation, daily, throughout the DSS-treatment, animals were monitored for weight loss, stool consistency and blood in the faeces (scale of 0-3). Histological score (0–3 scale) was based on destruction of epithelium, dilatation of crypts, loss of goblet cells, inflammatory cell infiltrate and oedema (Supplementary Fig. 2).

Human tissue samples

Embedded-paraffin sections of: i) colon of patients with mild and severe ulcerative colitis, ii) non-adenomatous colon polyps, iii) colon adenocarcinoma and iv) healthy colon located away from the adenocarcinoma region, were obtained from 25 patients (5 patients per each condition), between 49- and 74-year-old, who had undergone colon resection, through the ”Biobanco del Sistema Sanitario Público de Andalucía, Hospital Universitario Virgen del Rocío, Sevilla, Spain”. Tissues were subjected to a pathological examination at the Hospital to confirm the diagnosis of the pathology. The study was approved by the Ethic Committees of Sevilla University and of Virgen del Rocío Hospital. Informed consent was obtained from all patients.

Immunofluorescence assays

Immunofluorescence was performed on: i) mice ileum and colon, ii) colon from untreated and DSS-treated mice, iii) healthy colon, ulcerative colitis, non-adenomatous polyps and adenocarcinoma samples from patients, and iv) transfected Caco-2 cells. Transfected Caco-2 cells were grown on glass coverslips for 3 days and fixed directly in methanol at −20 °C for 10 min. 5 µm-paraffin embedded intestinal slides were boiled with 10 mM

sodium citrate, pH 6, during 10 min. After blocking the intestinal sections for 1h (3% bovine serum albumin, BSA; 3% fetal calf serum, and 0.1% triton x100 in PBS) and the Caco-2 cells for 10 min (0.5% BSA and 20 mM glycine in PBS), they were incubated either without (controls) or with the primary antibody at 4 °C, overnight. In the intestinal samples the primary antibody binding was visualized with the appropriate secondary antibodies: either Alexa Fluor -488 (1:100, Invitrogen) or -546 (1:100, Life technologies), and in Caco-2 cells with either FITC or Cy3 (1:500, Jackson ImmunoResearch Inc.). Nuclei were stained with Hoechst 33258 (Invitrogen). The intestinal slides were mounted (Vectashield, Vector) and photographed with an Olympus BX61 microscope equipped with a DP73 camera. Coverslips containing the Caco-2 cells were mounted (ProLong Gold, Invitrogen) and visualized with a DMIRB Leica microscope with a camera (C4742-95, Hamamatsu Photonics). Images were analysed using NIH ImageJ program. Quantification of colocalization was done by 3 independent observers by counting the total number of cells in 12 crypts well oriented longitudinally per sample and number of cells with yellow-orange colour signal per crypt. The results are expressed as the number of cells (either total or with yellow-orange colour signal) per crypt. The immunofluorescence intensity signal of Dab2 and E-cadherin was measured in 12 crypts well oriented longitudinally per sample and the results are expressed in arbitrary units. Negative controls without primary antibody were run in parallel (supplementary Fig. 3)

Western blot assays

Caco-2 cell were collected by washing twice with PBS and after SDS-PAGE sample buffer addition, the cells were homogenized with a 23G needle and heated at 70°C for 10 minutes. Samples were then processed using standard western blotting techniques. Protein-bound antibodies were detected with horseradish peroxidase conjugated secondary antibodies using enhanced chemiluminescence detection system (GE Healthcare Select®). Anti-α-tubulin antibody was used to normalize band density values.

Statistical analysis

Data are presented as mean ± SEM. The number of animals or patients used for each condition was 5. One way ANOVA followed by Tukey´s test was used for multiple comparisons (GraphPad Prism Program v8.0). For comparisons between two groups, Student´s *t* test was used. Differences were set to be significant for $p<0.05$.

Results

Localization of Dab2 in the small and large intestine of suckling and adult mice

In the current work we investigated Dab2 function in adult mouse and human intestine under physiological and physiopathological conditions. We started the work determining by immunofluorescence the location of Dab2 protein in colon of 8 day- and 3 month-old mice and comparing the observations with those obtained in the ileum. As previously, in the suckling ileum the anti-Dab2 antibody specific signal was strong at the apical membrane of the cells lining the villus (Fig.1). In the adult ileum, Dab2 signal was seen at both apical and lateral cell membranes of the villus and crypt cells. The absence of Dab2 signal at the lateral cell membrane of suckling intestine might be due to the strong apical signal that precludes emerging the much less strong signals from the lateral membrane.

In the suckling and adult colon, Dab2 signal is mainly at the lateral membranes of the crypt cells, being the signal intensity stronger at the bottom of the crypts. The colonocytes apical membrane was slightly stained mainly in the suckling mice. The results suggest that the main function of Dab2 in adult intestinal epithelial is related to lateral membrane processes.

Dab2 depletion disrupts epithelial cell-cell apical junctions

As Dab2 was detected at the epithelial lateral membrane we tested whether it regulates the AJC by silencing its gene expression (siDab2) in Caco-2 cells (siRNA technique) and analysing the expression (western blot) and location (immunofluorescence) of TJ (ZO-1 and occludin) and AJ (E-cadherin and β-catenin) proteins. The western blot revealed that the silencing procedure reduced the expression of the two Dab2 isoforms by about 70% (Fig. 2a). Tight junction appearance, as detected by occludin and ZO-1 staining, changed from a linear organization into a wavy structure (Fig. 2b). In Dab2-containing Caco-2 cells, E-cadherin mainly appeared at the cell membrane as a linear structure and as a few E-cadherin spots in the cytoplasm. These spots likely might represent E-cadherin localization in cytosolic vesicles. Dab2 depletion affected E-cadherin membrane localization and increased its staining in the cytosol. This E-cadherin redistribution was accompanied by increases in cytosolic β-catenin (Fig. 2b). Western blots show that Dab2 depletion did not significantly changed the abundance of the AJC proteins assayed (Fig. 2c). These observations suggest that Dab2 is required for proper AJC organization, mainly AJs.

Since the observed siDab2-induced alterations in ZO-1 and occludin distribution might modify the barrier properties of the TJ, we next measured the TER and the paracellular dextran permeability in either control or siDab2 Caco-2 cells monolayers. Neither the TER nor the dextran permeability (Supplementary Fig. 1) were affected by siDab2, indicating that the AJC disruption induced by 70% Dab2 depletion is not big enough as to significantly modify the paracellular permeability.

Colocalization of Dab2 and E-cadherin in the small and large intestine of suckling and adult mice

The most prominent effect of siDab2 on Caco-2 cells AJC was the change in E-cadherin distribution; we next determined Dab2 and E-cadherin colocalization in mouse intestinal epithelium by immunofluorescence. In all the samples examined, the anti-E-cadherin antibody signal was seen at the lateral cell membranes (Fig. 3). Dab2 colocalized with E-cadherin at the cell lateral membrane in both, ileum and colon. In the suckling ileum colocalization was observed at the crypt-villus junction and along the crypt-villus axis in the adult. In both, suckling and adult colon, colocalization was mainly detected at the bottom of the crypts (Fig. 3). These observations suggest that, as in Caco-2 cells, in mouse intestinal epithelium the E-cadherin membrane location is related to Dab2.

DSS-treatment effects on the expression and localization of Dab2 and E-cadherin in mice colon

Since the available evidence indicates that mucosal inflammation induces E-cadherin downregulation or mislocalization, we evaluated, by immunofluorescence, whether inflammatory conditions (DSS-treatment during 3, 6 and 9 days) affected the colon expression and localization of Dab2 and E-cadherin. Supplementary Fig. 2 summarized the indicators of the colon inflammation progression. Inflammation was relevant by day 3 of DSS-treatment, though some of the inflammatory parameters were mildly increased. Compared with untreated colon, 6- and 9- days treatment increased the levels of the pro-inflammatory cytokines by about 100 and 1000 times, respectively.

As compared with DSS-untreated mice (see Fig.4), 3 days of DSS-treatment increased: i) the number of cells expressing Dab2 along the entire crypt (Fig. 4a); ii) the intensity of the Dab-2 and E-cadherin signals at the lateral cell membranes, cytosol and apical membrane domain (Fig. 4a and 4b), and iii) the number of crypt cells and colonocytes showing Dab2 and E-cadherin colocalization even at the apical membrane (Fig. 4a and 4c). Colocalization extends to about two-thirds of each crypt, instead of only at the bottom. After 6 days of DSS-treatment the normal structure of the colon epithelium

was destroyed (Fig. 4a) and therefore epithelial Dab2 and E-cadherin signal intensity was decreased (Fig. 4b). The remaining epithelium exhibited less Dab2 at the lateral membranes (Fig. 4a) and, consequently, decreased Dab2/E-cadherin colocalization (Fig. 4c). This colocalization was absent after 9 days of DSS-treatment (Fig. 4a). These observations might indicate that the intestine firstly responds to tissue injury by increasing epithelial Dab2 and E-cadherin to strengthen the AJC and hence provide protection against inflammation. After 9 days, the inflammatory inducers lead to depletion of epithelial Dab2 and E-cadherin.

Dab2 and E-cadherin localization in human healthy and pathological colon

We next determine whether the Dab2 and E-cadherin response to experimental colitis found in mice also occurs in human colon. Immunofluorescence was performed on colon specimens from patients with mild and severe ulcerative colitis, with non-adenomatous colon polyps and colon adenocarcinoma and from healthy colon. As in mouse colon, in human healthy colon Dab2 and E-cadherin are located at cell lateral membrane and both proteins colocalized mainly at the bottom of the crypts (Fig. 5). In mild ulcerative colitis specimens, the E-cadherin signal was found at the lateral cell membrane, at the apical membrane domain in some cells and in the cytosol; Dab2 signal was mainly at lateral membranes (Fig. 5). The intensity of both, Dab2 and E-cadherin signals were greater than in healthy colon (Fig. 7a) and the number of crypt cells showing Dab2 and E-cadherin colocalization was increased (Fig. 7b). In severe ulcerative colitis, expression and colocalization of Dab2 and E-cadherin is still higher than in healthy colon but only seen in those cells that still maintained the epithelial integrity (Fig 5, 7b and 7c).

Since ulcerative colitis is associated with increased risk of colon cancer development and Dab2 is considered to act as a tumour suppressor, we examined Dab2 localization in human colon polyps and adenocarcinomas. Polyp specimens (Fig. 6) showed strong Dab2, E-cadherin and Dab2/E-cadherin signals at the crypt cells lateral membranes and cytosol, higher than that in healthy colon and similar to that in colitis (Fig. 7). In the adenocarcinoma regions (Fig. 6) where the epithelium was partially preserved (adenocarcinoma 1), Dab2 and E-cadherin appeared as diffuse membranous and cytosolic signals surrounding the nucleus, being the E-cadherin signal at the membrane more abundant than that of Dab2. Some colocalization of Dab2 and E-cadherin was also observed. In other regions (adenocarcinoma 2), Dab2 was completely absent from the remaining epithelium-like structures whereas E-cadherin was still present. According to these observations, the disappearance of Dab2 from the intestinal epithelium precedes that of E-cadherin and these findings, together with those in a

mouse model of experimental colitis and Dab2-depleted Caco-2 cells, might suggest that the loss of Dab2 may lead to epithelial E-cadherin delocalization.

In 9 days DSS-treated mice colon, in human severe ulcerative colitis and colon adenocarcinoma, Dab2 is abundantly expressed by non-epithelial cells appearing in the mucosa and submucosa. Some of them are macrophages and lymphocytes as they present Dab2/arginase-1 colocalization (Supplementary Fig. 4).

Discussion

In the suckling rat ileum Dab2 localizes at the apical membrane domain and may participate in the endocytosis of milk components [14]. Herein we show that with age Dab2 localization shifts from the apical to the lateral epithelial cells membrane of mouse intestine, wherein it appears to contribute to AJC stability, which, in turn, might provide protection against intestinal pathology development. Thus, Dab2 is required for the proper AJs organization in Caco-2 cells, it co-localizes with E-cadherin at the cell-cell junctions in mice and human intestinal epithelium and its expression and colocalization with E-cadherin in colon is modified by pathological conditions.

TJs and AJs are dynamic structures that are remodelled in a variety of physiological and pathological situations, and their stability is critical to allow physiological compartmentalization and targeted during disease. Our data are the first demonstration of Dab2 localization at the AJC *ex vivo* and that Dab2 depletion induces E-cadherin internalization in Caco-2 cells. Consequently, E-cadherin delocalization was accompanied by β-catenin internalization. Dab2 depletion mildly affected TJs because, though it induces a loss of tension of the ZO-1 and occludin, TJ permeability was not affected. The small response of TJs to Dab2 depletion might indicate that either Dab2 is not important for TJ or that 70% Dab2 depletion was no enough to modify the TJs.

Inflammation increases AJC proteins endocytosis and decreases their exocytosis to the lateral cell membrane but mechanisms poorly understood (see [3] for review). Our results agree with those showing mislocalization of E-cadherin during intestinal inflammation (see [3] for review) and suggest that Dab2 is involved in this mislocalization. At the early stages of inflammation (3 days DSS-treatment), the colon responds to DSS-injury by increasing the intensity of Dab2 and E-cadherin signals and the number of epithelial cells co-expressing the two proteins at the lateral membrane. Coexpression of the two proteins is also observed at the apical membrane domain of epithelial cells. Yang et al. (2007) [18] proposed that directional transport and removal of apical E-cadherin by Dab2-mediated endocytosis is important for bilateral targeting. According to this proposal, our results suggest that at the beginning tissue injury increases the synthesis

of Dab2 and E-cadherin that were initially exported to the apical membrane, from where E-cadherin would be removed and targeted to the lateral membrane by Dab2- mediated endo/exocytosis. The increase in epithelial Dab2 and E-cadherin could be an initial tissue response to strengthen the AJs and hence, attempt to provide protection against colon inflammation. Accordingly, an inflammation-protecting role could be attributed to epithelial Dab2. Progression of mouse colon inflammation, from 3 to 6 and 9 days-treatment, is accompanied by epithelial Dab2 and E-cadherin downregulation, decreased Dab2/E-cadherin colocalization (6 days-treatment) and eventually absence of both, epithelial Dab2 and E-cadherin at 9 days-treatment.

Human inflamed colon and polyps exhibited increased Dab2/E-cadherin colocalization but progression to adenocarcinoma is accompanied either by loss of epithelial Dab2 and delocalization of E-cadherin. Therefore, as in rodents, human colon initially responds to damage by increasing Dab2/E-cadherin colocalization. In control conditions Dab2/E-cadherin colocalization is mainly observed at the bottom of the crypts, where the stem cells are located. Once the new cells established E-cadherin-mediated contacts, cell proliferation is stopped (see [19] for review). Hence, by contributing to the proper E-cadherin location at the cell-cell junction, Dab2 might regulate cell proliferation/differentiation transition. The observations made in Caco-2 cells corroborate this point of view and all together, the current findings are consistent with a role of Dab2 in the proper E-cadherin location at the cell-cell junction, thus maintaining the junction stability and the intestinal epithelium integrity and cell differentiation. Thus, Dab2 down-regulation produces loss of epithelial polarity during embryo development and carcinogenesis [18, 20–22] and correlates with EMT [11–13]. This role of Dab2 in epithelial polarity has been proposed as an underlying mechanism for its tumour-suppressive function (see [6] for review).

Progression of mice and human colon disorders, here studied, led to the appearance of non-epithelial cells expressing Dab2, which might represent immune cells, such as macrophages and lymphocytes. Upregulation of Dab2 in immune cells has been found under inflammatory conditions in other tissues [23–27].

In conclusion, as far as we know, this is the first report showing localization of Dab2 at the intestinal epithelium junctions *ex vivo* and that its specific depletion in culture cells led to E-cadherin internalization. Furthermore, our colitis model and pathological human tissue results also suggest a functional link between Dab2 and E-cadherin and that Dab2 might exert a protective function against mice colitis and human ulcerative colitis and cancer.

Acknowledgements

Immunohistochemistry images were obtained in the “Centro de Investigación Tecnología e Innovación de la Universidad de Sevilla” (CITIUS), Universidad de Sevilla. We also thank ”Biobanco Hospital Virgen del Rocío-IBIS (Biobanco SSPA y Red de Biobanco-ISCCII-PT13/0010/0056)” for providing us the human samples.

Funding information

The work was supported by a Grant from the Junta de Andalucía (CTS 5884) and by a fellowship from The European Molecular Biology Organization (EMBO; ASTF45-2012) to M.D. Vazquez-Carretero.

References

1. Pawłowska B, Prof. Sobieszczańska B (2017) Intestinal epithelial barrier: The target for pathogenic Escherichia coli. Adv Clin Exp Med 26:1437–1445. https://doi.org/10.17219/acem/64883

2. Miyoshi J, Takai Y (2005) Molecular perspective on tight-junction assembly and epithelial polarity. Adv Drug Deliv Rev 57:815–855. https://doi.org/10.1016/j.addr.2005.01.008

3. Lechuga S, Ivanov AI (2017) Disruption of the epithelial barrier during intestinal inflammation: Quest for new molecules and mechanisms. Biochim Biophys Acta - Mol Cell Res 1864:1183–1194. https://doi.org/10.1016/j.bbamcr.2017.03.007

4. Fukui H (2016) Increased Intestinal Permeability and Decreased Barrier Function: Does It Really Influence the Risk of Inflammation? Inflamm Intest Dis 1:134–145. https://doi.org/10.1159/000447252

5. Xu XX, Yang W, Jackowski S, Rock CO (1995) Cloning of a novel phosphoprotein regulated by colony-stimulating factor 1 shares a domain with the Drosophila disabled gene product. J Biol Chem 270:14184–14191. https://doi.org/10.1074/jbc.270.23.14184

6. Finkielstein C V., Capelluto DGS (2016) Disabled-2: A modular scaffold protein with multifaceted functions in signaling. BioEssays 38:S45-55. https://doi.org/10.1002/bies.201670907

7. Piehl M, Lehmann C, Gumpert A, et al (2006) Internalization of Large Double-Membrane Intercellular Vesicles by a Clathrin-dependent Endocytic Process. Mol Biol Cell 18:337–347. https://doi.org/10.1091/mbc.e06-06-0487

8. Rula ME, Cai KQ, Moore R, et al (2007) Cell autonomous sorting and surface positioning in the formation of primitive endoderm in embryoid bodies. Genesis 45:327–338. https://doi.org/10.1002/dvg.20298

9. Penheiter SG, Deep Singh R, Repellin CE, et al (2010) Type II Transforming Growth Factor- Receptor Recycling Is Dependent upon the Clathrin Adaptor Protein Dab2. Mol Biol Cell 21:4009–4019. https://doi.org/10.1091/mbc.e09-12-1019

10. Kleeff J, Huang Y, Mok SC, et al (2002) Down-regulation of DOC-2 in colorectal cancer points to its role as a tumor suppressor in this malignancy. Dis Colon Rectum 45:1242–1248. https://doi.org/10.1007/s10350-004-6399-2

11. Martin JC, Herbert BS, Hocevar BA (2010) Disabled-2 downregulation promotes epithelial-to-mesenchymal transition. Br J Cancer 103:1716–1723. https://doi.org/10.1038/sj.bjc.6605975

12. Piao J, You K, Guo Y, et al (2017) Substrate stiffness affects epithelial-mesenchymal transition of cervical cancer cells through miR-106b and its target protein DAB2. Int J Oncol 50:2033–2042. https://doi.org/10.3892/ijo.2017.3978

13. Chao A, Lin CY, Lee YS, et al (2012) Regulation of ovarian cancer progression by microRNA-187 through targeting Disabled homolog-2. Oncogene 31:764-775. https://doi.org/10.1038/onc.2011.269

14. Vázquez-Carretero MD, García-Miranda P, Calonge ML, et al (2011) Regulation of Dab2 expression in intestinal and renal epithelia by development. J Cell Biochem 112:354–361. https://doi.org/10.1002/jcb.22931

15. Elbediwy A, Zihni C, Terry SJ, et al (2012) Epithelial junction formation requires

confinement of Cdc42 activity by a novel SH3BP1 complex. J Cell Biol 198:677–693. https://doi.org/10.1083/jcb.201202094

16. Matter K, Balda MS (2003) Functional analysis of tight junctions. Methods. 30:228-234. https://doi.org/10.1016/S1046-2023(03)00029-X

17. Carvajal AE, Vazquez-Carretero MD, Garcia-Miranda P, et al (2017) Reelin expression is up-regulated in mice colon in response to acute colitis and provides resistance against colitis. Biochim Biophys Acta 1863:462–473. https://doi.org/10.1016/j.bbadis.2016.11.028

18. Yang DH, Cai KQ, Roland IH, et al (2007) Disabled-2 is an epithelial surface positioning gene. J Biol Chem 169:258–267. https://doi.org/10.1074/jbc.M611356200

19. Mendonsa AM, Na TY, Gumbiner BM (2018) E-cadherin in contact inhibition and cancer. Oncogene 37:4769-4780. https://doi.org/10.1038/s41388-018-0304-2

20. Yang DH, Smith ER, Roland IH, et al (2002) Disabled-2 is essential for endodermal cell positioning and structure formation during mouse embryogenesis. Dev Biol 251:27–44. https://doi.org/10.1006/dbio.2002.0810

21. Yang DH, Fazili Z, Smith ER, et al (2006) Disabled-2 heterozygous mice are predisposed to endometrial and ovarian tumorigenesis and exhibit sex-biased embryonic lethality in a p53-Null background. Am J Pathol. 169:258-267. https://doi.org/10.2353/ajpath.2006.060036

22. Moore R, Cai KQ, Tao W, et al (2013) Differential requirement for Dab2 in the development of embryonic and extra-embryonic tissues. BMC Dev Biol. 13:39. https://doi.org/10.1186/1471-213X-13-39

23. Moon C, Lee J, Ahn M, Shin T (2005) Involvement of Disabled-2 protein in the central nervous system inflammation following experimental cryoinjury of rat brains. Neurosci Lett. 378:88-91. https://doi.org/10.1016/j.neulet.2004.12.016

24. Jokubaitis VG, Gresle MM, Kemper DA, et al (2013) Endogenously regulated Dab2 worsens inflammatory injury in experimental autoimmune encephalomyelitis. Acta Neuropathol Commun. 1:32. https://doi.org/10.1186/2051-5960-1-32

25. Ahn M, Moon C, Park C, et al (2015) Transient activation of an adaptor protein, disabled-2, in rat spinal cord injury. Acta Histochem 117:56–61. https://doi.org/10.1016/j.acthis.2014.11.001

26. Ahmed MS, Byeon SE, Jeong Y, et al (2015) Dab2, a negative regulator of DC immunogenicity, is an attractive molecular target for DC-based immunotherapy. Oncoimmunology 4:e984550. https://doi.org/10.4161/2162402X.2014.984550

27. Adamson SE, Griffiths R, Moravec R, et al (2016) Disabled homolog 2 controls macrophage phenotypic polarization and adipose tissue inflammation. J Clin Invest 126:1311–1322. https://doi.org/10.1172/JCI79590

Legends

Fig. 1 Immunolocalization of Dab2 in the ileum and colon of suckling (8-day-old) and adult (3-month-old) mice. 5 µm tissue sections were incubated with anti-Dab2 (Santa Cruz, red) antibody. Dab2 localization at apical membrane (arrowheads) or at the junctions (small arrows) are pointed. Scale bars represent 50 µm. The photographs are representative of five different assays for each condition. See Materials and Methods for specific details.

Fig. 2 Effects of Dab2 depletion on expression and location of tight- and adherens-junctions proteins. Caco-2 cells transfected with either non-targeting (control) or siRNAs directed against Dab2 (siDab2) were used. A, Effect of Dab2 silencing on the Dab2 protein abundance analysed by Western blot; an anti-Dab2 antibody (BD Transduction Laboratories) was used. B, immunofluorescence and C, Western-blots using antibodies against the indicated proteins. α-tubulin was used as standard. Histograms represent the relative abundance of protein. The values represent means ± SEM of arbitrary units of protein abundance, Student´s *t* test: *p<0,05 *vs* control. Scale bars represent 10 µm. The photographs are representative of five different assays. See Materials and Methods for specific details.

Fig.3. Immunolocalization of Dab2 and E-cadherin in the ileum and colon of suckling (8-day-old) and adult (3-month-old) mice. 5 µm tissue sections were incubated with anti-Dab2 (Santa Cruz, red) and anti-E-cadherin (green) antibodies. Nuclei were visualized with Hoechst (blue). Dab2 localization at the apical membrane (arrowheads) or at the junctions (small arrows) are pointed. Yellow-orange colour indicates colocalization of both proteins (pointed with large arrows). Scale bars represent 50 µm. The photographs are representative of five different assays. See Materials and Methods for specific details.

Fig. 4 Effect of inflammation on Dab2 and E-cadherin location in the mice colon. 5 µm colon sections of 3 month-old mice without and with 3, 6 or 9 days DSS-treatment were incubated with anti-Dab2 (Santa Cruz, red) and anti-E-cadherin (green) antibodies. Nuclei were visualized with Hoechst (blue). Yellow-orange colour indicates colocalization of the both proteins under study (pointed with arrows). A, Representative photographs of five different immunohistochemistry assay. Scale bars represent 50 µm. Histograms represent means ± SEM of B, Dab2 or E-cadherin immunofluorescence intensity per crypt and C, Each bar represents the total number of cells per crypt and the number of cells having Dab2/E-cadherin colocalization per crypt. One-way ANOVA showed an

effect of inflammation progression on Dab2 and E-cadherin immunofluorescence intensity and Dab2/E-cadherin colocalization per crypt ($p<0.01$). Tukey's test: [a]$p<0.01$, DSS-treated *vs* untreated mice; [b]$p<0.01$, 6 days DSS-treated *vs* 3 days DSS-treated mice. Five mice were used per condition. See Materials and Methods for specific details.

Fig. 5 Immunolocalization of Dab2 and E-cadherin in human colon under inflammation conditions. 5-10 µm colon sections from human specimens of: healthy colon, mild ulcerative colitis and severe ulcerative colitis, were incubated with anti-Dab2 (Proteintech, red) and anti-E-cadherin (green) antibodies. Nuclei were visualized with Hoechst (blue). Yellow-orange colour indicates colocalization of the both proteins under study (pointed with arrows). Representative photographs of the immunohistochemistry assay are shown. Scale bars represent 50 µm. Five specimens were used per condition. See Materials and Methods for specific details.

Fig. 6 Immunolocalization of Dab2 and E-cadherin in human colon polyps and adenocarcinomas. 5-10 µm colon sections from human specimens of: non-adenomatous polyps and adenocarcinoma were incubated with anti-Dab2 (Proteintech, red) and anti-E-cadherin (green) antibodies. Nuclei were visualized with Hoechst (blue). Dab2 localization at the membrane (arrowheads) or at the cytosol (small arrows) are pointed. Yellow-orange colour indicates colocalization of the both proteins under study (pointed with large arrows). Scale bars represent 50 µm. Representative photographs of the immunohistochemistry assay are shown. Healthy colon is shown in Fig. 5. Adenocarcinomas labelled as 1 or 2 indicate two different representative areas within the same adenocarcinoma specimen. Five specimens were used per condition. See Materials and Methods for specific details.

Fig. 7 Quantification of immunofluorescence intensity and Dab2/E-cadherin colocalization in human colon specimens. Histograms represent means ± SEM. A, Dab2 or E-cadherin immunofluorescence intensity per crypt and B, Each bar represents the total number of cells per crypt and the number of cells having Dab2/E-cadherin colocalization per crypt. UC: ulcerative colitis. One-way ANOVA showed an effect of inflammation progression on Dab2 and E-cadherin immunofluorescence intensity and Dab2/E-cadherin colocalization per crypt ($p<0.01$). Tukey's test: [a]$p<0.01$, UC *vs* healthy colon; [b]$p<0.01$, severe UC *vs* mild UC or polyps *vs* mild UC. Five specimens were used per condition. See Materials and Methods for specific details.

Supplementary Fig. 1. Effects of Dab2 depletion on paracellular and ion permeability. A, Paracellular tracer permeability was measured on Caco-2 cells using fluorescently

labelled dextrans of 4 and 70 kDa. B, Transepithelial Electrical Resistance (TER) was measured on Caco-2 cells for a period of 24, 30, 48 and 60 hours culture. Data are means ± SEM, n=3.

Supplementary Fig. 2 Evaluation of the DSS-induced colitis progression. DSS (dextran sulphate sodium) was administered in the drinking water during either 3, 6 or 9 days as described in Methods. The following inflammation indicators are displayed: DAI, histological score of colon, representative photographs of H&E stained distal colon sections and mRNA relative abundance of IL-1β and TNF-α. Scale bars represent 100 µm. Data are means ± SEM. The number of animals used in each experimental condition was 5. Student's *t*-test: *p<0.001, **p<0.05, DSS-treated *vs*. untreated mice.

Supplementary Fig. 3. Negative controls of immunofluorescence assays. 5-10 µm ileum and colon sections from either mouse or patient specimens used in figures 1 and 3-6 were incubated without primary antibody but with the anti-rabbit IgG Alexa fluor-546 secondary antibody (Life technologies). Scale bars represent 50 µm. The photographs are representative of five different assays.

Supplementary Fig. 4. Immunolocalization of Dab2 and arginase-1. The colon of 9 days DSS-treated mice and of the human specimens (severe ulcerative colitis or adenocarcinoma) were utilized. 5-10 µm sections of the specimens were incubated with anti-Dab2 (either Santa Cruz for mouse or Proteintech for human samples, red) and anti-arginase-1 (green) antibodies. Nuclei were visualized with Hoechst (blue). Yellow-orange colour indicates colocalization of the both proteins under study (pointed with arrows). Scale bars represent 50 µm. The photographs are representative of five different.

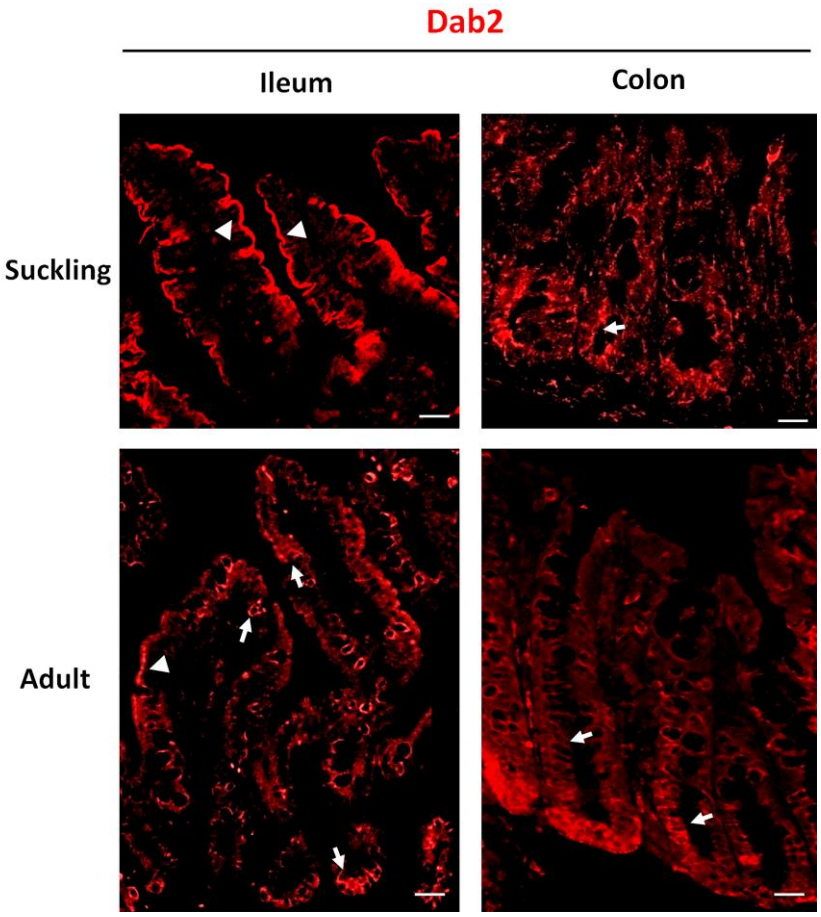

Fig. 1

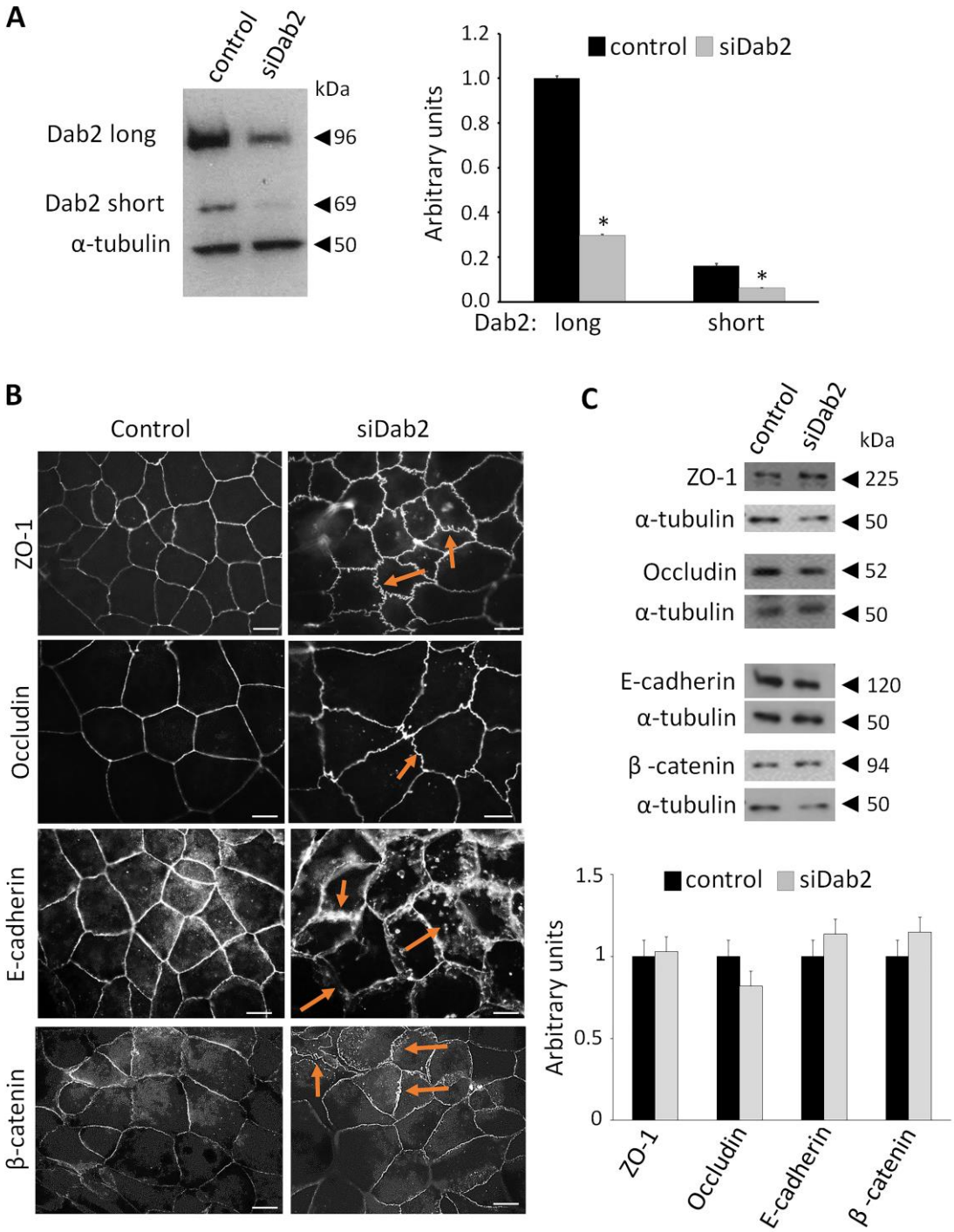
A
control
siDab2
kDa
Dab2 long
96
Dab2 short
69
α-tubulin
50
control
siDab2
Arbitrary units
1.2
1.0
0.8
0.6
0.4
0.2
0.0
*
*
Dab2: long
short
B
Control
siDab2
ZO-1
Occludin
E-cadherin
β-catenin
C
control
siDab2
kDa
ZO-1
225
α-tubulin
50
Occludin
52
α-tubulin
50
E-cadherin
120
α-tubulin
50
β -catenin
94
α-tubulin
50
control
siDab2
Arbitrary units
1.5
1
0.5
0
ZO-1
Occludin
E-cadherin
β -catenin

Fig.2

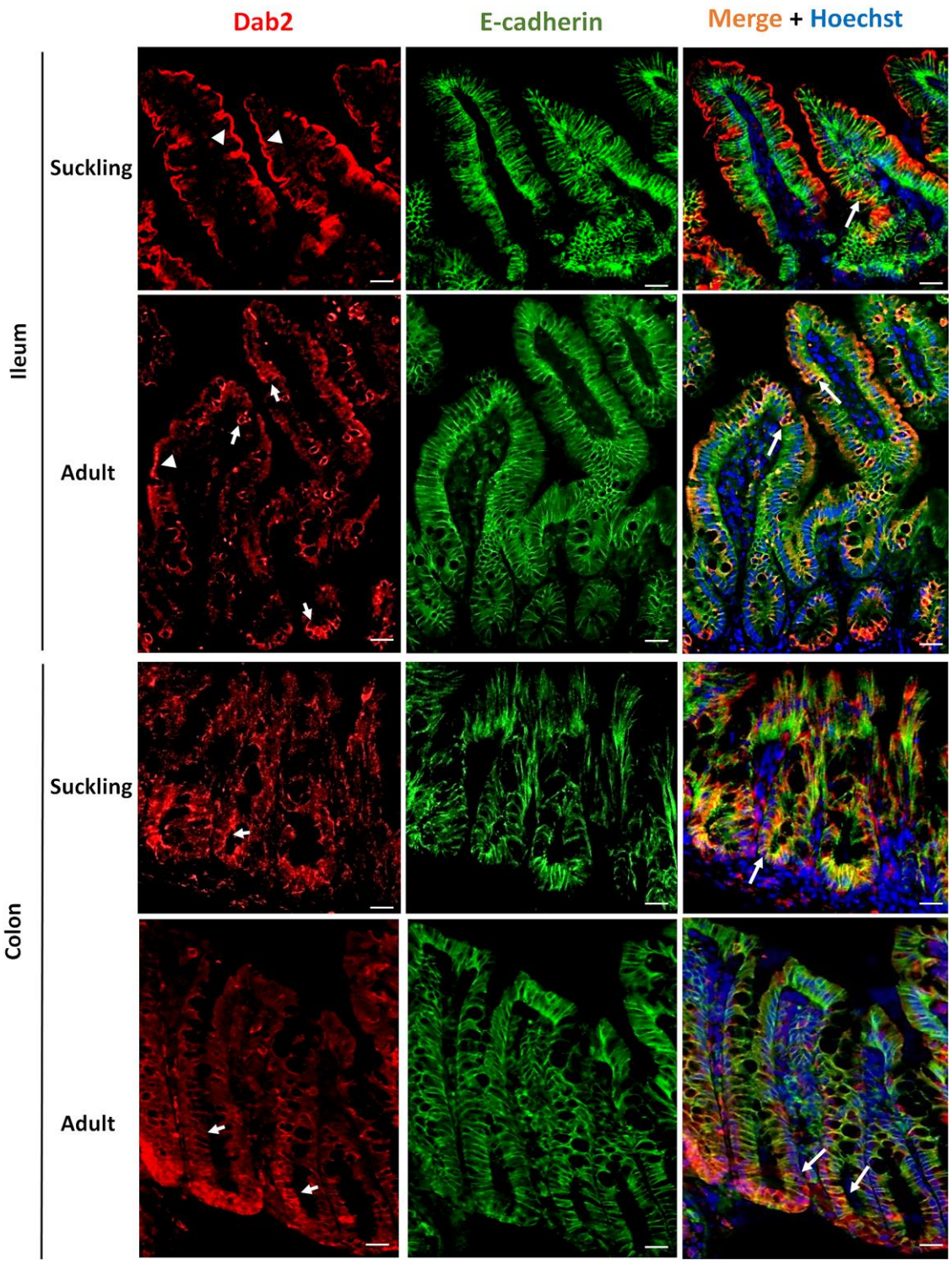
Dab2
E-cadherin
Merge + Hoechst
Ileum
Suckling
Adult
Colon
Suckling
Adult

Fig. 3

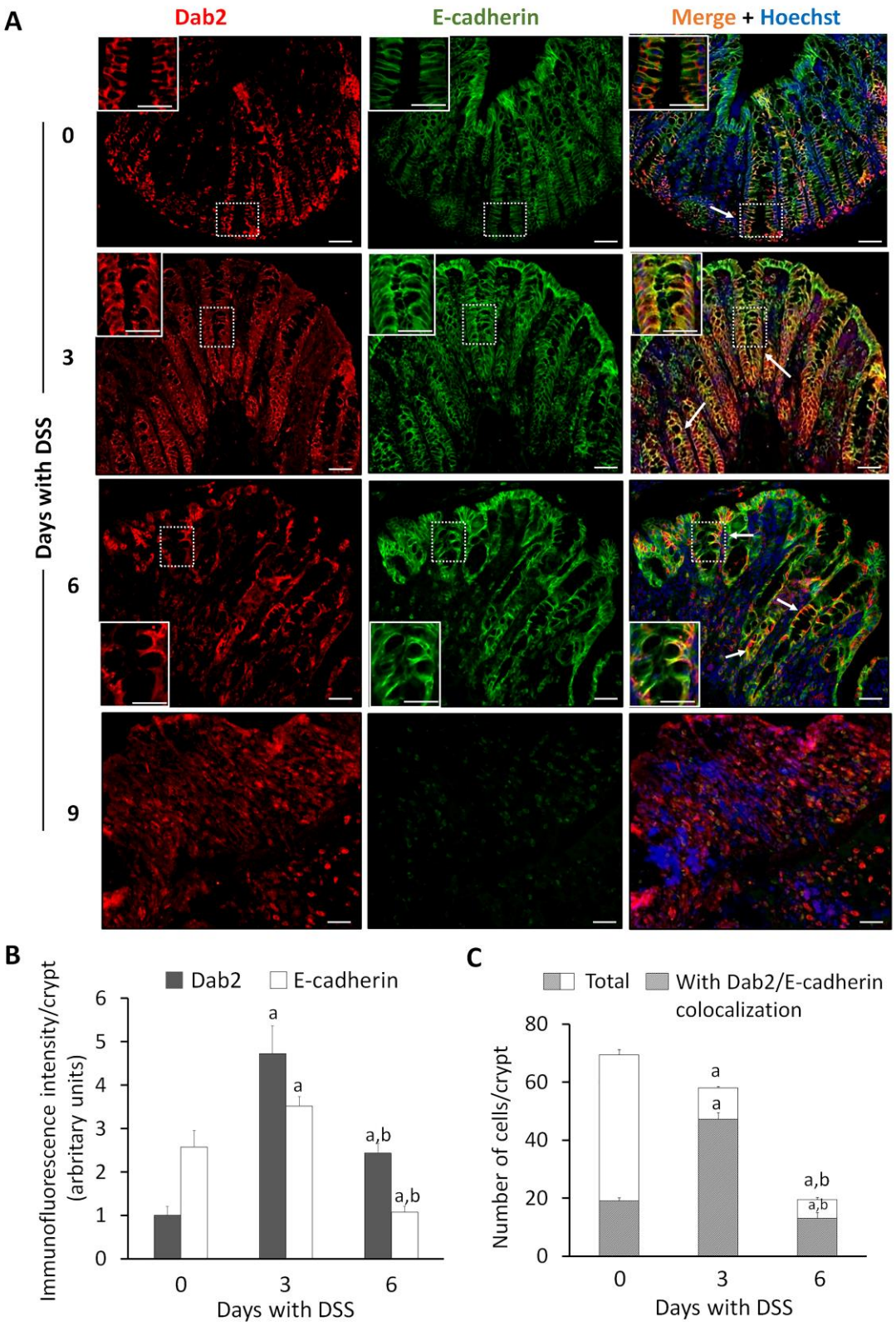
A
Dab2
E-cadherin
Merge + Hoechst
0
3
6
9
Days with DSS
B
Dab2
E-cadherin
Immunofluorescence intensity/crypt (arbritary units)
0
1
2
3
4
5
6
a
a
a,b
a,b
0
3
6
Days with DSS
C
Total
With Dab2/E-cadherin colocalization
Number of cells/crypt
0
20
40
60
80
a
a
a,b
a,b
0
3
6
Days with DSS

Fig. 4

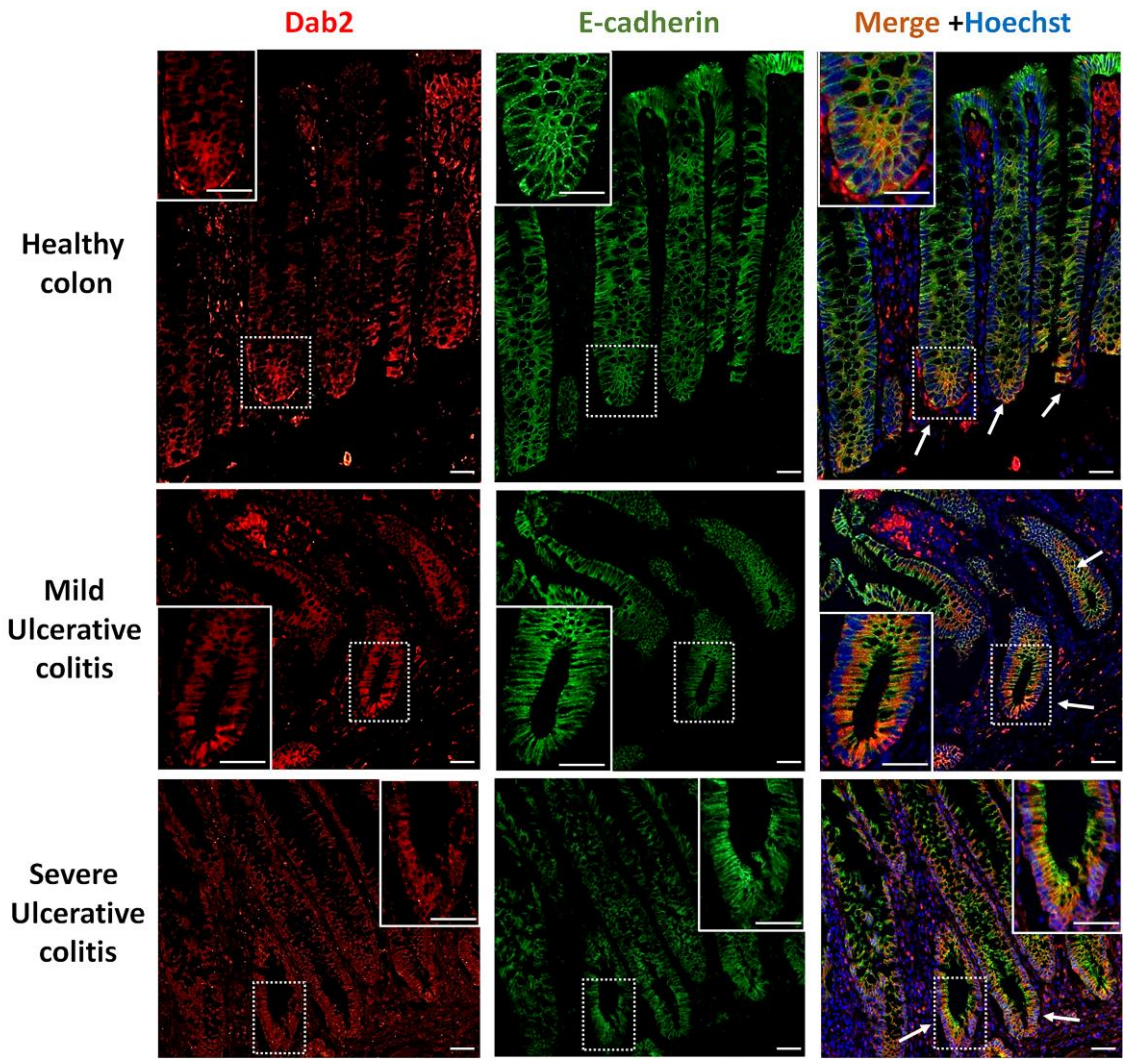
Dab2
E-cadherin
Merge +Hoechst
Healthy colon
Mild Ulcerative colitis
Severe Ulcerative colitis

Fig. 5

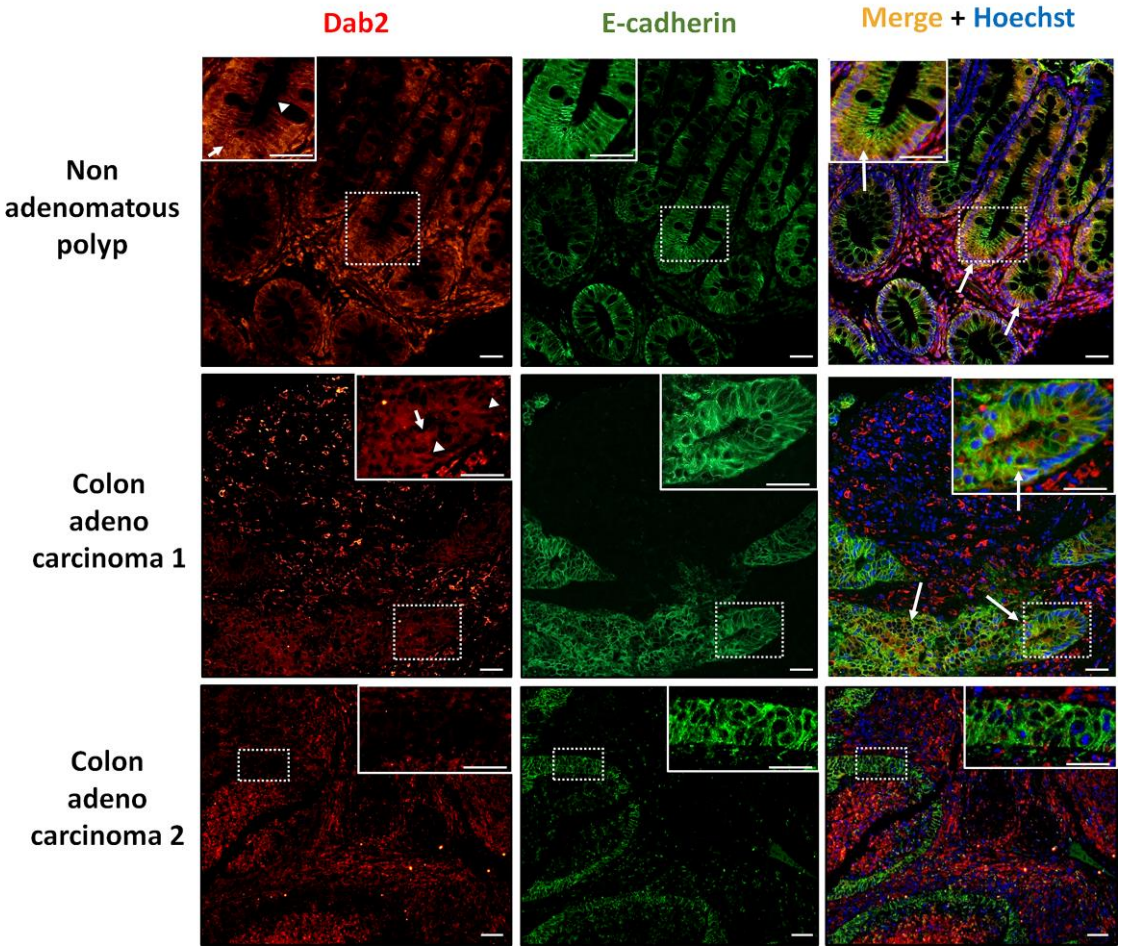
Dab2
E-cadherin
Merge + Hoechst
Non adenomatous polyp
Colon adeno carcinoma 1
Colon adeno carcinoma 2

Fig.6

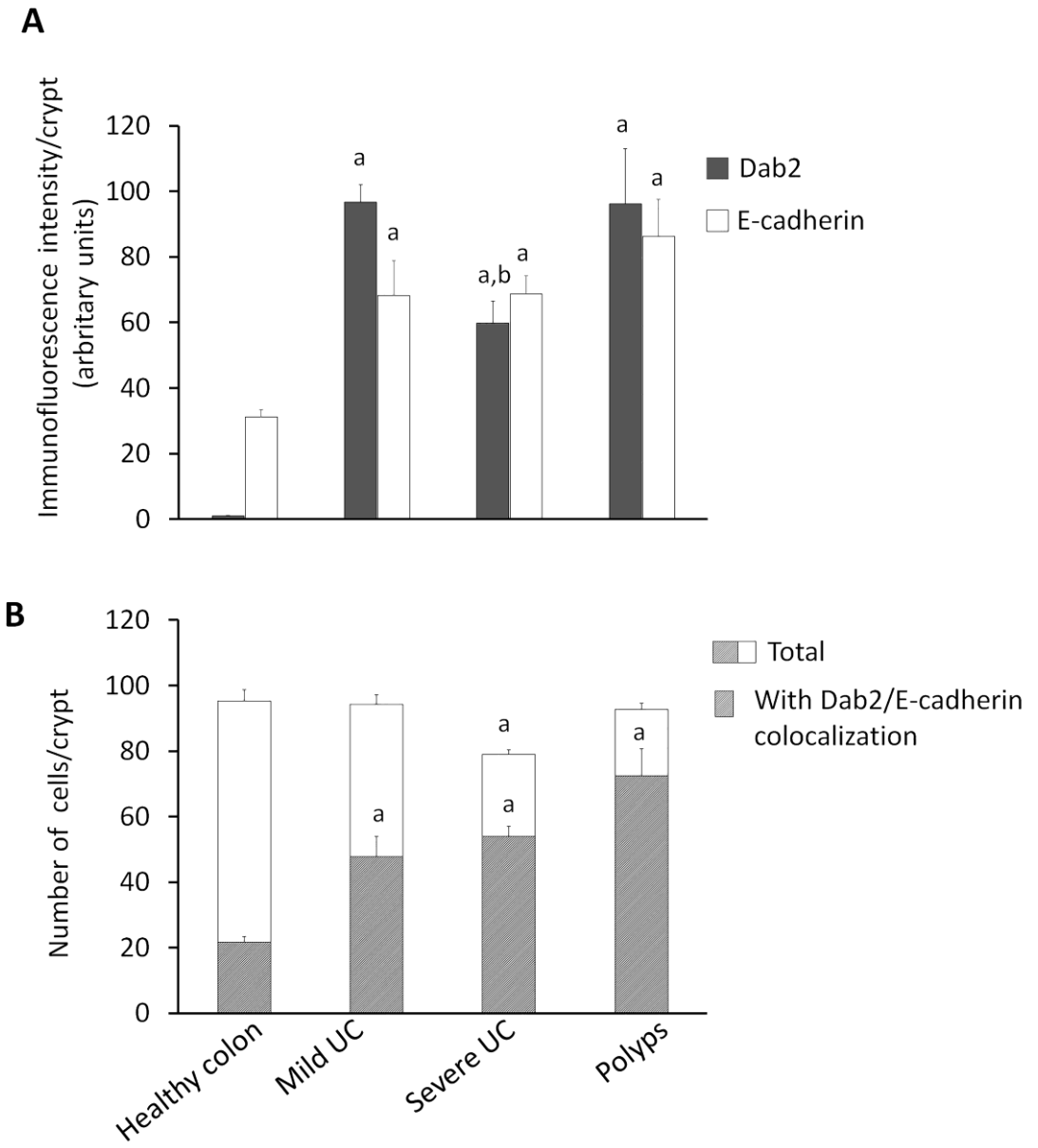
A
Immunofluorescence intensity/crypt (arbritary units)
120
100
80
60
40
20
0
a
a
a,b
a
a
a
Dab2
E-cadherin
B
Number of cells/crypt
120
100
80
60
40
20
0
a
a
a
a
Total
With Dab2/E-cadherin colocalization
Healthy colon
Mild UC
Severe UC
Polyps

Fig.7

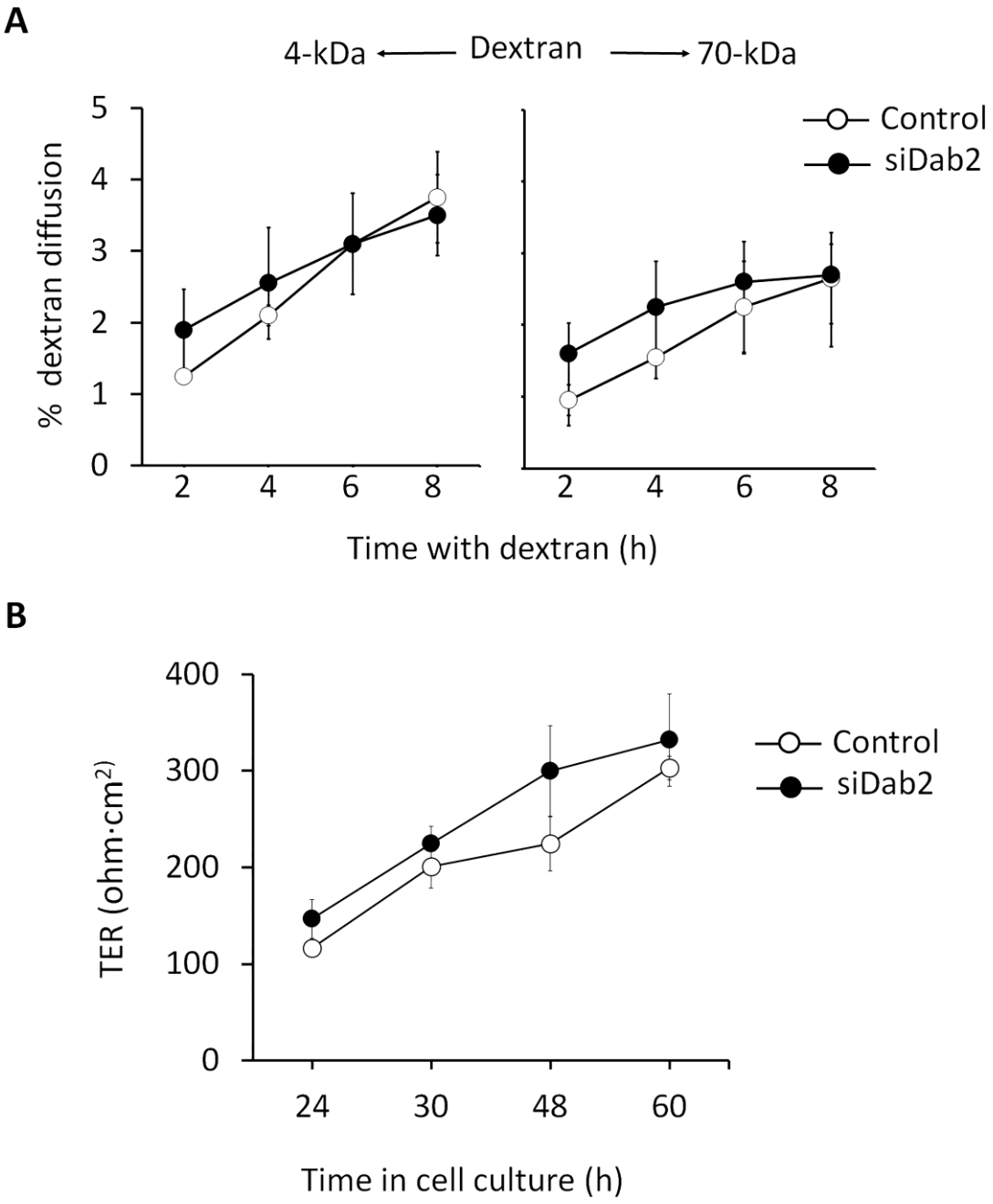
A
4-kDa
Dextran
70-kDa
% dextran diffusion
0
1
2
3
4
5
2
4
6
8
Control
siDab2
Time with dextran (h)
B
TER (ohm·cm²)
0
100
200
300
400
24
30
48
60
Control
siDab2
Time in cell culture (h)

Suppl. Fig. 1

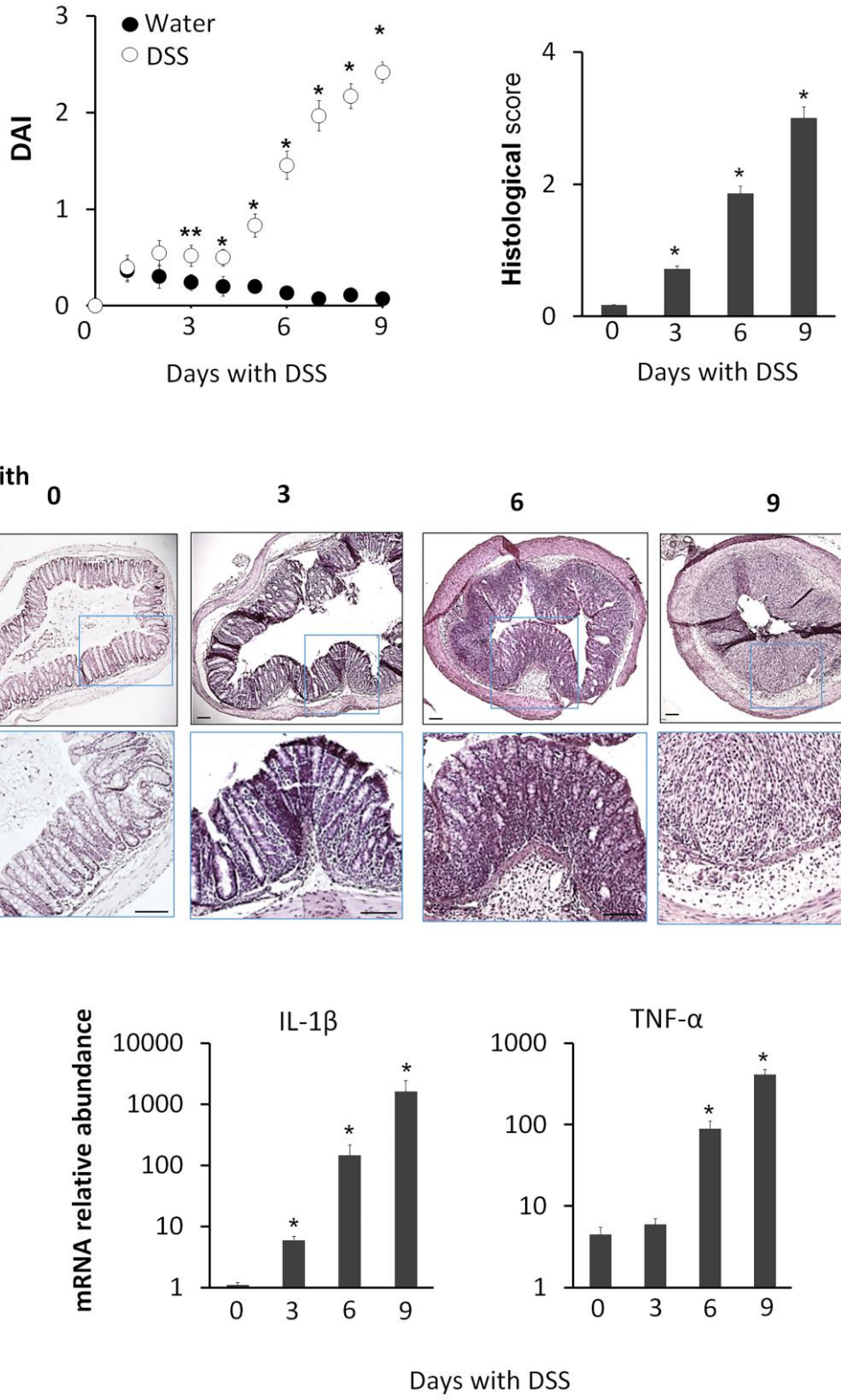
DAI
Water
DSS
Days with DSS
Histological score
Days with DSS
Days with DSS
0
3
6
9
mRNA relative abundance
IL-1β
TNF-α
Days with DSS

Supp. Fig. 2

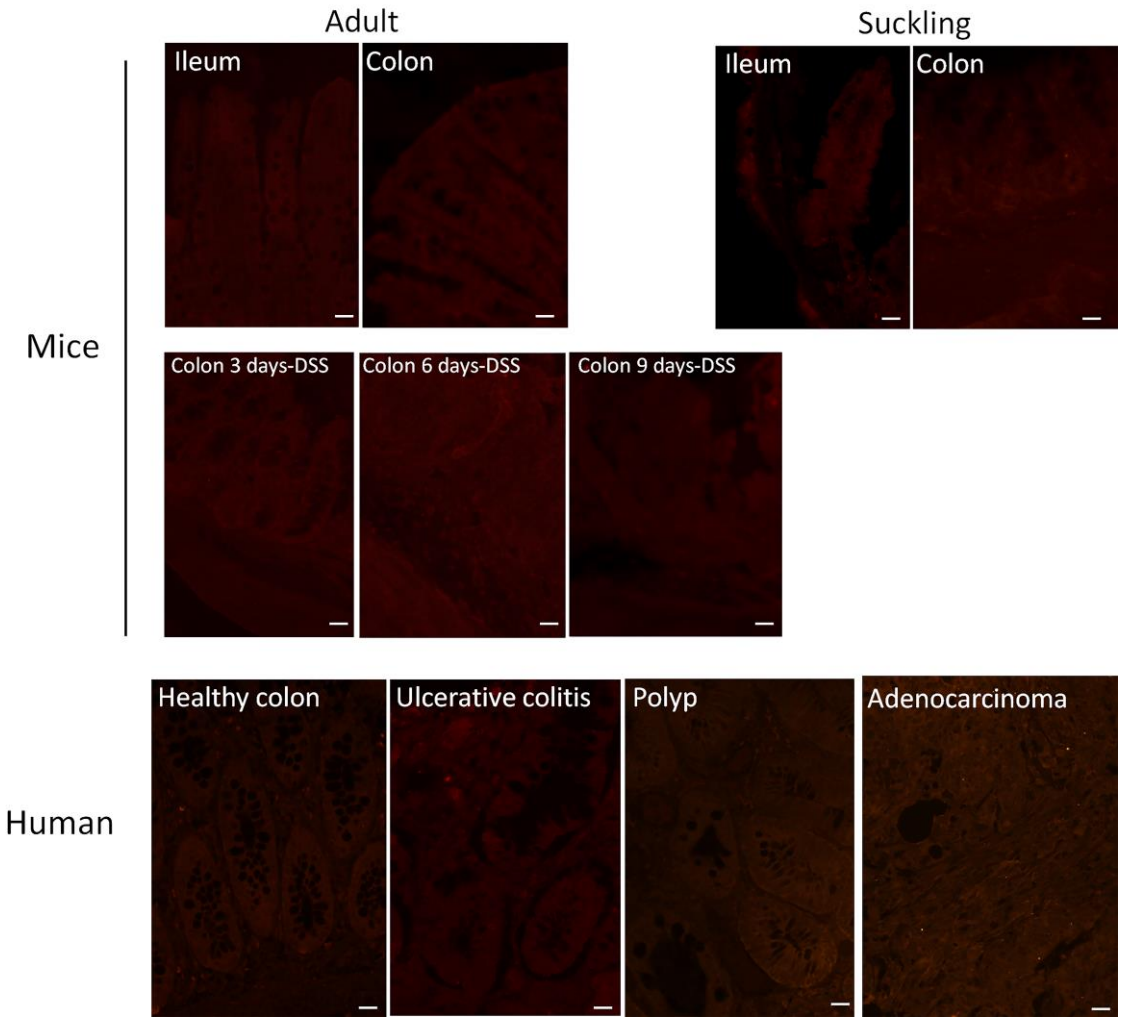
Adult
Suckling
Ileum
Colon
Ileum
Colon
Mice
Colon 3 days-DSS
Colon 6 days-DSS
Colon 9 days-DSS
Human
Healthy colon
Ulcerative colitis
Polyp
Adenocarcinoma

Supp. Fig. 3

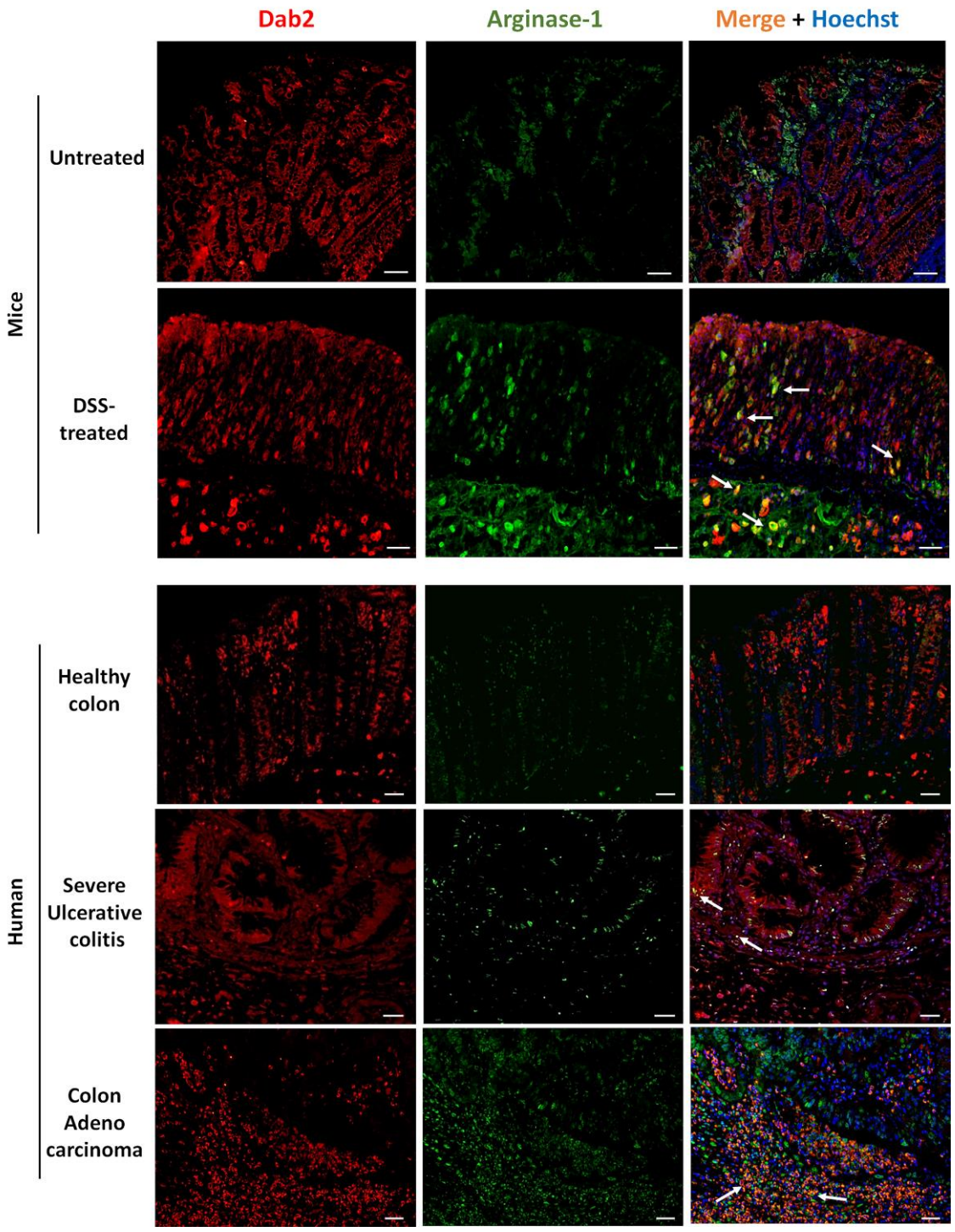
Dab2
Arginase-1
Merge + Hoechst
Mice
Untreated
DSS-treated
Human
Healthy colon
Severe Ulcerative colitis
Colon Adeno carcinoma

Supp. Fig.4